Clinical Correlates of Computationally Derived Visual Field Defect Archetypes in Patients from a Glaucoma Clinic

Sophie Cai[a], **Tobias Elze**[b,c], **Peter J. Bex**[b,d], **Janey L. Wiggs**[a], **Louis R. Pasquale**[a,e], **Lucy Q. Shen**[a]

[a]Department of Ophthalmology, Harvard Medical School, Massachusetts Eye and Ear, Boston, MA, USA;

[b]Department of Ophthalmology, Harvard Medical School, Schepens Eye Research Institute, Boston, MA, USA;

[c]Max Planck Institute for Mathematics in the Sciences, Leipzig, Germany;

[d]Department of Psychology, Northeastern University, Boston, MA, USA;

[e]Channing Division of Network Medicine, Brigham and Women's Hospital, Boston, MA, USA

Abstract

Purpose: To assess the clinical validity of visual field (VF) archetypal analysis, a previously developed machine learning method for decomposing any Humphrey VF (24−2) into a weighted sum of clinically recognizable VF loss patterns.

Materials and Methods: For each of 16 previously identified VF loss patterns ("archetypes," denoted AT1 through AT16), we screened 30,995 reliable VFs to select 10–20 representative patients whose VFs had the highest decomposition coefficients for each archetype. VF global indices and patient ocular and demographic features were extracted retrospectively. Based on resemblances between VF archetypes and clinically observed VF patterns, hypotheses were generated for associations between certain VF archetypes and clinical features, such as an association between AT6 (central island, representing severe VF loss) and large cup-to-disk ratio (CDR). Distributions of the selected clinical features were compared between representative eyes of certain archetypes and all other eyes using the two-tailed *t*-test or Fisher exact test.

Results: 243 eyes from 243 patients were included, representative of AT1 through AT16. CDR was more often ≥ 0.7 among eyes representative of AT6 (central island; $p = 0.002$), AT10 (inferior arcuate defect; $p = 0.048$), AT14 (superior paracentral defect; $p = 0.016$), and AT16 (inferior paracentral defect; $p = 0.016$) than other eyes. CDR was more often < 0.7 among eyes representative of AT1 (no focal defect; $p < 0.001$) and AT2 (superior defect; $p = 0.027$), which was also associated with ptosis ($p < 0.001$). AT12 (temporal hemianopia) was associated with history

of stroke ($p = 0.022$). AT11 (concentric peripheral defect) trended toward association with trial lens correction $> 6D$ ($p = 0.069$).

Conclusions: Shared clinical features between computationally derived VF archetypes and clinically observed VF patterns support the clinical validity of VF archetypal analysis.

Keywords

Archetype; glaucoma; machine learning; statistical models; visual field

Introduction

Visual field (VF) assessment is integral to the diagnosis and monitoring of glaucoma.[1] VF defects have traditionally been classified using a combination of qualitative descriptors[2] and quantitative and semi-quantitative summary indices reflecting VF loss severity, focality, and probability of glaucomatous etiology, such as mean deviation (MD), pattern standard deviation (PSD), and the Glaucoma Hemifield Test (GHT).[3] Clinical practice and research could benefit from the development of a unified quantitative VF classification system that: (1) is auto-mated, rapid, and reproducible, (2) simultaneously classifies information about the qualitative pattern and quantitative severity of VF loss, and (3) can be used to decompose complex VF defects into multiple components (potentially caused by different etiologies) that can be independently tracked over time.

Toward the goal of developing such a quantitative VF classification and monitoring system, Elze et al.[4] applied the machine learning method of archetypal analysis to a large database of reliable Humphrey VF (24–2) total deviation plots from a glaucoma practice. Archetypal analysis, first developed by Cutler and Breiman,[5] is an established computational method for (1) discovering representative patterns ("archetypes") that emphasize distinguishing features of a heterogeneous dataset (e.g., of VF total deviation plots) and (2) quantitatively decomposing any member of the dataset into a weighted sum of each of the identified archetypes. A detailed comparison of archetypal analysis to alternative quantitative VF classification approaches has been previously discussed by Elze et al.[4] In brief, one alternative approach is prototype analysis, such as k-means clustering, in which a set of VFs is divided into clusters by similarity, and representative patterns ("prototypes") are defined as the centers (means) of these clusters. VF archetypal analysis, in contrast, identifies archetypes at the tails rather than centers of the VF distribution, more explicitly highlighting distinctive features of VF loss than prototype analysis. While k-means clustering results in assignment of any VF to exactly one cluster (represented by its prototype), archetypal analysis represents any VF as a weighted combination of archetypes, which is particularly relevant to clinical settings where multiple types of VF loss potentially contribute to a patient's overall VF pattern.

Using archetypal analysis, Elze et al. derived an optimal representation of any Humphrey VF (24–2) total deviation plot as a weighted sum of 17 VF archetypes, hereafter denoted AT1 through AT17 (Figure 1). Notably, with the exception of the clinically insignificant overfit AT17 (mathematically required to ensure that the coefficients of archetypes always sum to 1),[4] VF archetypes that were derived computationally without clinician input remarkably

resemble clinically observed qualitative VF patterns, such as those previously described and categorized according to clinical significance by Keltner et al.[6] in the Ocular Hypertension Treatment Study. Compared to less clinically recognizable VF patterns derived from alternative computational approaches such as *k*-means clustering, VF archetypes may be more amenable to clinical correlation and application.

Before VF archetypal analysis can be fully utilized, this novel quantitative VF classification system needs clinical validation. Based on the resemblance between computationally derived VF archetypes and clinically recognized qualitative VF patterns, we hypothesized that VF archetypes share clinical phenotypes with the qualitative VF patterns that they resemble – confirmation of which would support the clinical interpretability of computationally derived VF archetypes and their potential application to patient care. The aim of the present study was to test for associations between representative eyes of certain VF archetypes and clinical features known to be associated with the qualitative VF patterns that the archetypes resemble.

Materials and methods

This study was approved by the Massachusetts Eye and Ear Institutional Review Board and conducted in accordance with the ethical tenets of the Declaration of Helsinki. 30,995 reliable (fixation loss rate 33% and false-positive and false-negative rates 20%; criteria selected for consistency with Elze et al.[4]) Humphrey VFs (24–2 Swedish Interactive Threshold Algorithms Standard) recorded between January 2007 and October 2013 were retrospectively collected from the Humphrey Field Analyzers II (Carl Zeiss Meditec AG, Jena, Germany) at the Massachusetts Eye and Ear Glaucoma Service. Each VF was represented as a weighted sum of VF archetype coefficients using the previously described VF archetypal decomposition algorithm[4] (Figure 2). With an initial minimum cutoff of archetype coefficient 0.7, up to 20 representative eyes from adult patients (18 years of age) were selected for each of AT1 through AT16 by identifying eyes whose VFs had the highest decomposition coefficients of each archetype. AT17 was excluded as clinically insignificant. The minimum archetype coefficient was lowered as needed (not below 0.5) to ensure inclusion of at least 10 representative eyes per archetype. For a patient whose both eyes had high coefficients of either the same or different archetypes, only the eye whose VF had the higher archetype coefficient was included. Representative eyes of AT6 (central island) were selected to have best corrected visual acuity (BCVA) of 20/50 or better at the time of the corresponding VF. VFs were also manually reviewed to confirm qualitative consistency with the results of VF archetypal decomposition, as well as to check for reproducibility of VF defect patterns when multiple VFs over time were available.

We retrospectively extracted VF global indices from the Humphrey VF plots and patient ocular and systemic features from electronic medical record clinic notes from the dates of the selected VFs. For an eye with multiple VFs with high coefficients of a given archetype, the earliest-dated VF with coefficient 0.7 was selected to better capture chronological associations between archetypes and certain clinical features. The clinical features included in analysis were selected based on expected relevance to known glaucomatous and nonglaucomatous etiologies of the qualitative VF patterns that the VF archetypes resemble.

Clinical data that were not consistently documented (e.g., maximum known intraocular pressure) were excluded from analysis. Glaucoma diagnoses were recorded from clinician assessments, except for eyes with AT1 (no focal defect), which were at most considered as corresponding to glaucoma suspect status due to the absence of VF loss. Cup-to-disk ratios (CDRs) were recorded from clinician assessments, as optic disk photographs were not consistently available for confirmation. To supplement CDR analysis, a glaucoma specialist (LQS) masked to archetype assignment graded optic disk photographs that were available within 24 months of the corresponding VFs as glaucomatous, borderline glaucomatous, or non-glaucomatous. Grading criteria for glaucomatous optic nerve appearance included subjective assessment of CDR ⩾ 0.7 adjusted for disk size, focal neuroretinal rim thinning or notching, retinal vessel changes including bayoneting, presence of disk hemorrhages, and focal retinal nerve fiber layer loss. History of stroke was recorded from chart-documented past medical history, as confirmatory brain imaging was not consistently available.

Descriptive statistics were generated for baseline characteristics of representative eyes of each archetype. To assess for reproducibility of the VF archetypal decomposition algorithm in identifying representative VFs with similar severity and distribution of VF loss, we tested for basic expected correlations between VF archetypes and VF global indices, as well as for homogeneity of VF MD and PSD. We also identified other clinical features that we expected to be associated with certain VF archetypes (e.g., we expected AT6 (central island) to be associated with large CDR and glaucomatous optic nerve appearance on disk photograph) and compared the distribution of the selected characteristic for representative eyes of the given archetype with that for representative eyes of all other archetypes combined. A value of $p < 0.05$ was used to identify statistically significant differences using the two-tailed Student's t-test or Fisher exact test for continuous or categorical data, respectively. All analyses were performed using the Stata statistical package, version 12.1 (StataCorp LP, College Station, TX, USA).

Results

243 eyes in total were included as representative of AT1 through AT16. Table 1 summarizes the minimum archetype coefficients as well as VF indices and ocular and demographic features of representative eyes of each archetype. 154 eyes (63.4%) had multiple VFs available and were confirmed to have reproducible VF defects by both qualitative inspection and quantitative confirmation of a consistent dominant archetype in archetypal decomposition.

The overall mean MD for the included VFs was −11.0 ± 8.7 dB (Table 1). The mean MD was most positive among VFs representative of AT1 (no focal defect; 2.0 ± 1.0 dB) and most negative among VFs representative of AT6 (central island; −31.5 ± 1.6 dB), AT8 (superior altitudinal defect; −14.8 ± 1.5 dB), AT13 (inferior altitudinal defect; −19.5 ± 1.8 dB), AT11 (concentric peripheral defect; −17.0 ± 2.7 dB), AT12 (temporal hemianopia; −14.9 ± 2.0 dB), and AT15 (nasal hemianopia; −18.5 ± 2.7 dB). The overall mean PSD was 9.5 ± 4.1 dB. The mean PSD was lowest among VFs representative of AT1 (no focal defect; 1.6 ± 0.3 dB) and AT6 (central island; 4.1 ± 1.8 dB).

Table 1 and Figure 3 summarize the CDR distributions for representative eyes of each archetype. We hypothesized that representative eyes of glaucomatous- and non-glaucomatous-appearing VF archetypes would be more and less likely, respectively, to be associated with CDR 0.7. Eyes representative of several archetypes resembling glaucomatous VF defect patterns were significantly more likely to have CDR 0.7 than other eyes: AT6 (central island; 90.0% vs. 55.3%; $p = 0.002$), AT10 (inferior arcuate defect; 90.0% vs. 56.8%; $p = 0.048$), AT14 (superior paracentral defect;87.5% vs. 56.1%; $p = 0.016$), and AT16 (inferior paracentral defect;91.7% vs. 56.4%; $p = 0.016$). For a few other archetypes resembling glaucomatous VF loss, there were nonsignificantly higher percentages of eyes with CDR 0.7 than for other archetypes: AT8 (superior altitudinal defect; 80.0% vs. 56.2%; $p = 0.056$), AT13 (inferior altitudinal defect; 70.0% vs. 57.1%; $p = 0.345$), and AT3 (superior nasal step; 70.0% vs. 57.1%; $p = 0.345$). AT5 (inferior nasal step) was not associated with a higher percentage of eyes with CDR 0.7 (52.6% vs. 58.6%; $p = 0.635$). Meanwhile, the percentage of eyes with CDR 0.7 was significantly lower among eyes representative of AT1 (no focal defect; 5.0% vs. 63.0%; $p < 0.001$) and AT2 (superior defect; 31.6% vs. 60.5%; $p = 0.027$) than among other eyes. The lower percentage of eyes with CDR 0.7 trended toward statistical significance for AT11 (concentric peripheral defect; 30.0% vs. 59.4%; $p = 0.099$), but was not significant for AT12 (temporal hemianopia; 54.5% vs. 58.3%; $p = 1.000$) or AT15 (nasal hemianopia: 55.6% vs. 58.3%; $p = 1.000$).

179 eyes (73.7%) had disk photographs available within 24 months of the corresponding VF (Table 1). For 122 eyes (50.2% of the total cohort), disk photographs were available within 6 months of the corresponding VF. Representative eyes of the following archetypes were significantly more likely than other eyes to have glaucomatous optic nerve appearance on disk photo-graph: AT3 (superior nasal step; 83.3% vs. 49.7%; $p = 0.011$), AT6 (central island; 87.5% vs. 49.7%; $p = 0.004$), AT8 (superior altitudinal defect; 100.0% vs. 49.1%; $p < 0.001$), and AT16 (inferior paracentral defect; 88.9% vs. 51.2%; $p = 0.038$). The higher percentage of representative eyes with glaucomatous optic nerve appearance trended toward statistical significance for AT14 (superior paracentral defect; 78.6% vs. 50.9%; $p = 0.054$). Representative eyes of the following archetypes were significantly less likely to have glaucomatous optic nerve appearance on disk photograph: AT1 (no focal defect; 10.0% vs. 55.6%; $p = 0.007$) and AT11 (concentric peripheral defect; 0.0% vs. 55.6%; $p = 0.002$).

The mean BCVA was 0.1 ± 0.2 in logMAR notation for all archetypes combined, excluding AT6 (central island) because a BCVA-based inclusion criterion was used to select representative eyes for this archetype (Table 1). We tested whether the mean BCVA was significantly worse among eyes representative of AT7 (central scotoma) and AT13 (inferior altitudinal defect) than among other eyes, confirming statistically significant differences for both (AT7: 0.5 ± 0.4 vs. 0.1 ± 0.2; $p < 0.001$; AT13:0.4 ± 0.5 vs. 0.1 ± 0.2; $p < 0.001$). We assessed whether eyes representative of AT2 (superior defect) were more often associated with clinician-documented ptosis of the ipsilateral eyelid than other eyes, finding a statistically significant difference (60.0% vs. 9.0%; $p < 0.001$). We tested whether eyes representative of AT11 (concentric peripheral defect) were associated with a higher likelihood of requiring high hyperopic trial lens correction, finding a trend toward association (20.0% vs. 3.9% requiring trial lens correction > 6D; $p = 0.069$). Finally, we

tested whether patients whose eyes were representative of AT12 (temporal hemianopia) and AT15 (nasal hemianopia) were more likely to have a history of stroke than patients representative of other archetypes, finding a significant difference for the former (30.0% vs. 5.6%; $p = 0.022$) but not for the latter (10.0% vs. 6.5%; $p = 0.504$).

Discussion

In this study, we identified clinical correlates of several VF archetypes that are consistent with known associations for the corresponding qualitative VF patterns. Since VF archetypes were originally derived using a computational algorithm agnostic to clinical input, we first assessed for basic expected correlations between VF archetypes and global indices, as well as for similarities in MD and PSD among VFs representative of the same archetype. We found, as expected, that mean MD was least negative for VFs representative of AT1 (no focal defect) and most negative for VFs representative of archetypes with diffuse VF loss, such as AT6 (central island). Also consistent with expectations, mean PSD, a measure of focality of VF loss, was lowest among VFs representative of both normal (AT1; no focal defect) and globally depressed (AT6; central island) VF sensitivity.[7] The small standard deviations of MD and PSD for individual archetypes (< 2.8 dB and < 2.1 dB, respectively) support the homogeneity of representative VFs for each archetype.

CDR itself is a limited surrogate for glaucomatous optic nerve morphology as compared to more comprehensive optic nerve assessments such as the Disc Damage Likelihood Scale developed by Spaeth et al.[8–10] However, due to inconsistent availability of confirmatory structural data, we found in this retrospective study that clinician-documented CDR was the most uniformly available clinical parameter relevant to identification of glaucomatous optic nerve appearance. Applying the CDR 0.7 cutoff commonly reported in the literature for helping to distinguish between more and less likely glaucomatous optic disks,[11] we identified VFs representative of AT6 (central island), AT10 (inferior arcuate defect), AT14 (superior paracentral defect), and AT16 (inferior paracentral defect) as more likely than others to be glaucomatous, consistent with previous literature describing these VF defect patterns in eyes with glaucoma.[12] Also consistent with prior expectations, we identified VFs representative of AT1 (no focal defect) and AT2 (superior defect; also more specifically associated with ptosis[13]) as more likely than others to be nonglaucomatous. Review of available disk photographs for glaucomatous optic nerve appearance largely confirmed the findings from CDR analysis alone. The lack of association of AT13 (inferior altitudinal defect) with CDR 0.7 is consistent with the inclusion of nonglaucomatous causes of inferior altitudinal VF loss, such as nonarteritic anterior ischemic optic neuropathy.[14] The lack of association of AT5 (inferior nasal step) with CDR 0.7 or glaucomatous optic nerve appearance on disk photograph is corroborated by a previous report of a weaker association with abnormal optic disk morphology for peripheral nasal step than paracentral VF defects, [15] which may relate to a tendency of eyes with relatively pure nasal step defects to have earlier glaucomatous disease than eyes with other glaucomatous VF defects, as well as to the higher density of retinal ganglion cells in the central and paracentral than peripheral retina.[16]

Among other clinically expected associations were: the higher percentages of eyes representative of AT7 (central scotoma) and AT13 (inferior altitudinal defect) with worse

BCVA; the trend toward a higher percentage of eyes representative of AT11 (concentric peripheral defect) requiring high hyperopic VF trial lens correction, suggestive of lens rim artifact;[17] and the higher percentage of patients representative of AT12 (temporal hemianopia) with a history of stroke.[18] The absence of association between AT15 (nasal hemianopia) and history of stroke may be at least partly attributable to the smaller number of representative patients and lower minimum archetype decomposition coefficient for this archetype.

Our study has several limitations. Due to its retrospective nature, we could not establish causal relationships and did not have consistent access to documentation of some potentially valuable clinical and structural features, notably maximum intraocular pressure, refractive error, optic disk photographs, and optical coherence tomography data. Since patients included in this study were preferentially selected from a glaucoma clinic, history of stroke was defined by past medical history, with corresponding brain CT or MRI confirmatory imaging available in only four of 16 patients (25.0%). More consistent documentation of anatomic localization would enable better correlation with site of functional VF loss. Due to variability in patient follow-up, one third of VFs in this study did not have additional confirmatory VFs. Despite the relatively large overall sample size, the number of representative eyes per VF archetype was relatively small. For some archetypes, such as AT1 (no focal defect), the number of representative eyes was limited to 20 to achieve relatively even representation across archetypes. For other archetypes, not many VFs with high archetype decomposition coefficients were available. The lower representation of AT9 (inferotemporal defect), AT11 (concentric peripheral defect), and AT15 (nasal hemianopia) in our database can be attributed to the likely nonglaucomatous etiologies of these disorders, given that VFs included in the present study were obtained from a glaucoma practice. The limited number of VFs highly representative of AT15 (nasal hemianopia) was also partly due to overlap with other archetypes with nasal involvement such as AT5 (inferior nasal step) and AT10 (inferior arcuate defect), meaning that patients with partial nasal hemianopia may have mixed coefficients of several archetypes and thus not be as purely representative of AT15 (nasal hemianopia). Similarly, the limited number of VFs purely representative of AT10 (inferior arcuate defect) may be attributed to overlap of this archetype with AT5 (inferior nasal step) and AT13 (inferior altitudinal defect).

Despite these limitations, this study represents the first step toward clinical characterization and validation of computationally derived VF archetypes, supporting their further development for application to clinical practice and research. Compared to previous qualitative approaches to VF classification, VF archetypal analysis offers the advantage of reproducible quantitative decomposition of any VF into its multiple potential components, each of which may have a separate etiology (Figure 2b) and whose progression can be independently monitored over time. Assessing the clinical validity of VF archetypes among patients with similar severities of VF loss may permit further evaluation of the capacity of VF archetypal decomposition to discriminate between glaucomatous and non-glaucomatous VF loss and to distinguish different patterns of glaucomatous VF loss. Further refinement of the interpretation and monitoring of archetypal decomposition coefficients over time will be valuable for potential application of VF archetypal analysis as an aid to glaucoma diagnosis and progression detection. Finally, by facilitating rapid and reproducible screening of large

VF databases for subsets of VFs with desired characteristics, VF archetypal analysis has potential to help contribute to the advancement of VF research in glaucoma.

Funding

References

1. Brusini P, Johnson CA. Staging functional damage in glaucoma: review of different classification methods. Surv Ophthalmol 2007;52:156–179. [PubMed: 17355855]

2. Drance SM. The glaucomatous visual field. Br J Ophthalmol 1972;56:186–200. [PubMed: 5032754]

3. Asman P, Heijl A. Glaucoma hemifield test. Automated visual field evaluation. Arch Ophthalmol 1992;110:812–819. [PubMed: 1596230]

4. Elze T, Pasquale LR, Shen LQ, Chen TC, Wiggs JL, Bex PJ. Patterns of functional vision loss in glaucoma determined with archetypal analysis. J R Soc Interface 2015;12.

5. Cutler A, Breiman L. Archetypal analysis. Technometrics 1994;36: 338–347.

6. Keltner JL, Johnson CA, Cello KE, Edwards MA, Bandermann SE, Kass MA, et al. Classification of visual field abnormalities in the ocular hypertension treatment study. Arch Ophthalmol 2003;121:643–650. [PubMed: 12742841]

7. Blumenthal EZ, Sapir-Pichhadze R. Misleading statistical calculations in far-advanced glaucomatous visual field loss. Ophthalmology 2003;110:196–200. [PubMed: 12511366]

8. Chandra A, Bandyopadhyay AK, Bhaduri G. A comparative study of two methods of optic disc evaluation in patients of glaucoma. Oman J Ophthalmol 2013;6:103–107. [PubMed: 24082669]

9. Danesh-Meyer HV, Gaskin BJ, Jayusundera T, Donaldson M, Gamble GD. Comparison of disc damage likelihood scale, cup to disc ratio, and Heidelberg retina tomograph in the diagnosis of glaucoma. Br J Ophthalmol 2006;90:437–441. [PubMed: 16547323]

10. Spaeth GL, Henderer J, Liu C, Kesen M, Altangerel U, Bayer A, et al. The disc damage likelihood scale: reproducibility of a new method of estimating the amount of optic nerve damage caused by glaucoma. Trans Am Ophthalmol Soc 2002;100:181–185; discussion 185–186. [PubMed: 12545692]

11. Hollands H, Johnson D, Hollands S, Simel DL, Jinapriya D, Sharma S. Do findings on routine examination identify patients at risk for primary open-angle glaucoma? The rational clinical examination systematic review. JAMA. 2013;309:2035–2042. [PubMed: 23677315]

12. Park SC, De Moraes CG, Teng CC, Tello C, Liebmann JM, Ritch R. Initial parafoveal versus peripheral scotomas in glaucoma: risk factors and visual field characteristics. Ophthalmology 2011;118:1782–1789. [PubMed: 21665283]

13. Patipa M Visual field loss in primary gaze and reading gaze due to acquired blepharoptosis and visual field improvement following ptosis surgery. Arch Ophthalmol 1992;110:63–67. [PubMed: 1731724]

14. Han S, Jung JJ, Kim US. Differences between non-arteritic anterior ischemic optic neuropathy and open angle glaucoma with altitudinal visual field defect. Korean J Ophthalmol 2015;29:418–423. [PubMed: 26635459]

15. Jung KI, Park HY, Park CK. Characteristics of optic disc morphology in glaucoma patients with parafoveal scotoma compared to peripheral scotoma. Invest Ophthalmol Vis Sci 2012;53:4813–4820. [PubMed: 22714895]

16. Curcio CA, Allen KA. Topography of ganglion cells in human retina. J Comp Neurol 1990;300:5–25. [PubMed: 2229487]

17. Zalta AH. Lens rim artifact in automated threshold perimetry. Ophthalmology 1989;96:1302–1311. [PubMed: 2779998]

18. McAuley DL, Russell RW. Correlation of CAT scan and visual field defects in vascular lesions of the posterior visual pathways. J Neurol Neurosurg Psychiatry 1979;42:298–311. [PubMed: 458477]
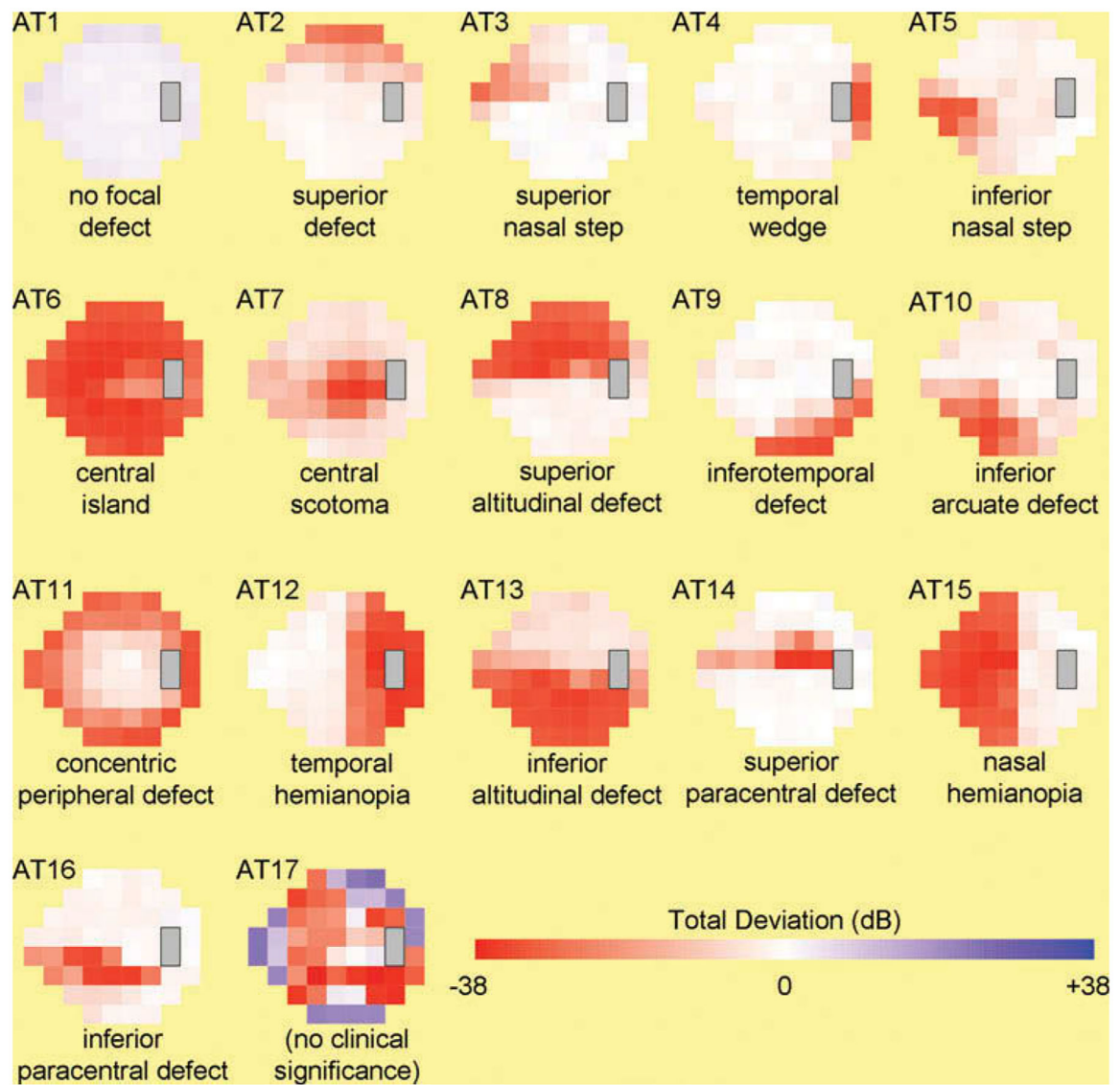
Figure 1.
Visual field archetypes identified from patients from a glaucoma clinic. Figure modified with permission from Elze et al.[4] Archetype (AT) patterns correspond to right-eye-formatted Humphrey Visual Field (24–2) total deviation plots. The two points closest to the blind spot were excluded from the 54 test points. Total deviations (measured in dB) reflect patient sensitivity threshold deviations as compared to age-matched normal subjects. Qualitative descriptors under each archetype pattern were assigned based on predominant regions of visual field loss; no descriptor is included under AT17, as this is a clinically insignificant overfit (see text for more details).
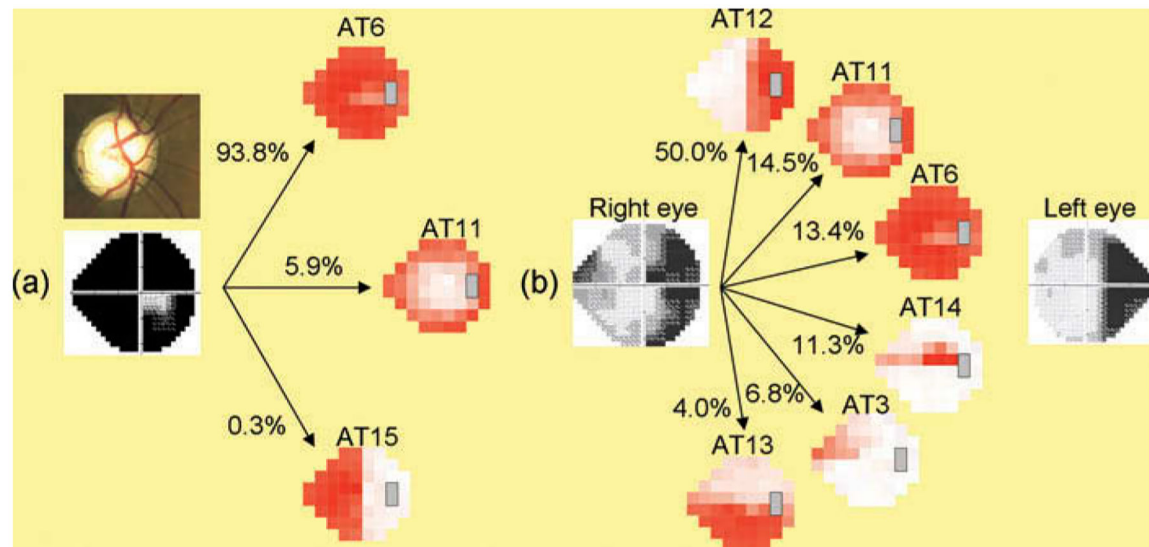
Figure 2.
Sample visual field archetypal decompositions. (a) Representative visual field archetypal decomposition (only showing archetypes with decomposition coefficients >0.1%) of a Humphrey Visual Field (24–2) test from the right eye of a 49-year-old African American man with advanced juvenile open angle glaucoma. This eye is representative of AT6 (central island), given the high decomposition coefficient of this archetype. The corresponding disk photograph above shows advanced cupping, despite which the best corrected visual acuity was 20/25. The mean deviation was −31.36 dB and the pattern standard deviation was 6.43 dB on Humphrey Visual Field testing. (b) Representative visual field archetypal decomposition (only showing archetypes with decomposition coefficients > 0.1%) of a Humphrey Visual Field (24–2) test from the right eye of an 84-year-old Caucasian woman with primary open angle glaucoma and history of stroke with residual right homonymous hemianopia. Archetypal decomposition quantitatively represents this complex visual field as a composite of multiple patterns, several of which were confirmed by reviewing the patient's clinical records. Specifically, archetypal analysis identifies the following nonglaucomatous components: AT12 (temporal hemianopia), consistent with a history of stroke and the corresponding nasal hemianopsia in the left eye visual field (shown at right for reference); and AT11 (concentric peripheral defect), consistent with clinical documentation of difficult positioning during examination. Archetypal decomposition also identifies the following glaucomatous components: AT6 (central island), AT14 (superior paracentral defect), AT3 (superior nasal step), and AT13 (inferior altitudinal defect). The physician-graded cup-to-disk ratio was 0.8. The mean deviation was −15.53 dB and the pattern standard deviation was 9.69 dB on Humphrey Visual Field testing.
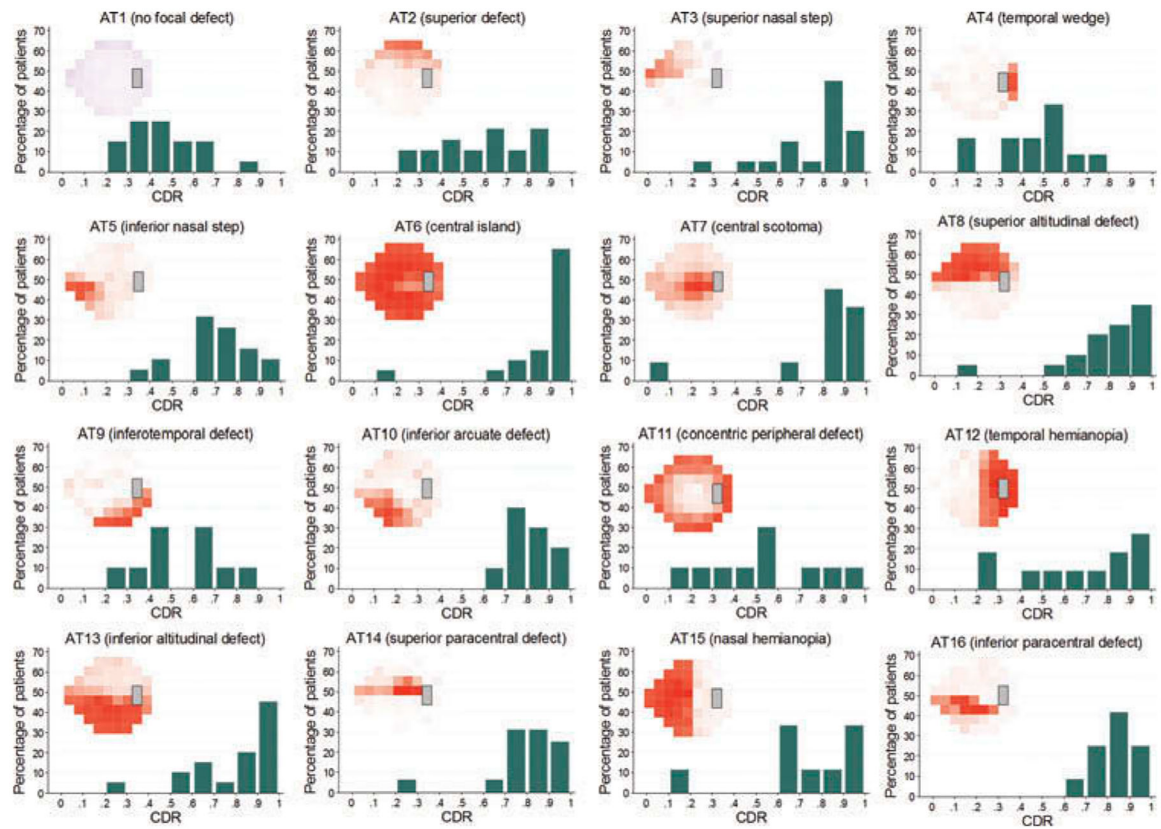
Figure 3.
Cup-to-disk ratio distributions by visual field archetype. Vertical axis: percentage of representative eyes for given archetype; horizontal axis: cup-to-disk ratio (CDR) in increments of 0.1. CDRs were obtained from clinic note attending assessments. Sample interpretation of continuous histogram distribution: for AT2 (superior defect), 10.0% of representative eyes had $0.2 \leq$ CDR < 0.3.

Table 1.

Baseline characteristics of study population stratified by archetype (AT).

	Total	AT1	AT2	AT3	AT4	AT 5	AT6	AT7	AT 8	AT9	AT10	AT11	AT 12	AT 13	AT14	AT15	AT16
Number of eyes	243	20	20	20	12	20	20	11	20	10	10	10	12	20	16	10	12
Lowest AT coefficient		0.96	0.77	0.80	0.71	0.71	0.94	0.70	0.84	0.65	0.67	0.67	0.75	0.78	0.70	0.53	0.72
Visual Field Indices																	
MD (dB: mean ± SD)	−11.0 ± 8.7	2.0 ± 1.0	−5.5 ± 1.3	−4.5 ± 1.5	−4.5 ± 2.4	−6.9 ± 1.7	−31.5 ± 1.6	−11.0 ± 2.4	−14.8 ± 1.5	−7.1 ± 1.5	−8.4 ± 1.5	−17.0 ± 2.7	−14.9 ± 2.0	−19.5 ± 1.8	−5.6 ± 2.3	−18.5 ± 2.7	−9.4 ± 2.5
PSD (dB: mean ± SD)	9.5 ± 4.1	1.6 ± 0.3	6.8 ± 1.6	8.0 ± 1.5	6.5 ± 1.1	8.9 ± 1.4	4.1 ± 1.8	11.3 ± 1.4	14.6 ± 1.3	11.1 ± 1.2	11.2 ± 1.7	11.4 ± 1.2	14.5 ± 0.9	13.3 ± 1.6	9.9 ± 0.8	14.0 ± 2.0	12.9 ± 1.0
Optic Nerve Features																	
CDR (mean ± SD)	0.7 ± 0.2	0.4 ± 0.2	0.5 ± 0.2	0.7 ± 0.2	0.4 ± 0.2	0.7 ± 0.2	0.8 ± 0.2	0.8 ± 0.3	0.8 ± 0.2	0.5 ± 0.2	0.8 ± 0.1	0.5 ± 0.3	0.6 ± 0.3	0.8 ± 0.2	0.8 ± 0.2	0.7 ± 0.3	0.8 ± 0.1
Number of eyes with disk photo within 24 months of VF (%)	179 (73.7)	10 (50.0)	15 (75.0)	18 (90.0)	8 (66.7)	15 (75.0)	16 (80.0)	7 (63.6)	14 (70.0)	9 (90.0)	7 (70.0)	8 (80.0)	6 (50.0)	17 (85.0)	14 (87.5)	6 (60.0)	9 (75.0)
Disk photo optic nerve appearance (% glaucomatous)[a]	53.1	10.0	33.3	83.3	12.5	33.3	87.5	71.4	100.0	11.1	57.1	0.0	16.7	47.1	78.6	33.3	88.9
Ocular Features																	
Glaucoma diagnosis (% POAG)	82.1	0.0[b]	76.5	80.0	80.0	78.9	72.2	80.0	88.2	85.7	100.0	77.8	100.0	77.8	75.0	88.9	100.0
Current IOP (mm Hg: mean ± SD)	15.3 ± 6.0	15.5 ± 3.5	14.7 ± 3.2	14.6 ± 2.9	14.6 ± 3.3	15.6 ± 5.1	21.4 ± 12.9	14.0 ± 4.2	13.8 ± 3.2	13.0 ± 2.1	13.9 ± 4.6	14.6 ± 3.0	16.2 ± 4.3	15.8 ± 9.8	14.1 ± 4.8	16.2 ± 4.1	15.0 ± 3.0
BCVA (logMAR: mean ± SD)	0.1 ± 0.2	0.0 ± 0.1	0.2 ± 0.2	0.1 ± 0.1	0.1 ± 0.1	0.1 ± 0.2	0.2 ± 0.2	0.5 ± 0.4	0.1 ± 0.1	0.1 ± 0.1	0.1 ± 0.1	0.2 ± 0.2	0.2 ± 0.1	0.4 ± 0.5	0.1 ± 0.1	0.1 ± 0.1	0.0 ± 0.1
Demographic Features																	
Age (years: mean ± SD)	61.7 ± 15.1	58.7 ± 9.9	72.6 ± 10.6	63.6 ± 15.6	68.0 ± 10.1	66.7 ± 10.1	48.0 ± 10.8	65.9 ± 10.0	58.0 ± 12.0	48.7 ± 22.7	60.6 ± 20.9	60.1 ± 16.8	59.4 ± 18.2	66.9 ± 19.0	62.7 ± 11.7	60.6 ± 17.2	61.7 ± 10.5
Sex (% male)	51.0	55.0	35.0	35.0	58.3	50.0	70.0	81.8	55.0	40.0	80.0	50.0	50.0	60.0	43.8	40.0	16.7
Race (% European ancestry)	71.4	66.7	80.0	85.0	72.7	78.9	15.0	81.8	73.7	50.0	80.0	90.0	75.0	57.9	87.5	77.8	91.7

Abbreviations: AT, archetype; MD, mean deviation; PSD, pattern standard deviation; CDR, cup-to-disk ratio; VF, visual field; POAG, primary open angle glaucoma; IOP, intraocular pressure; BCVA, best corrected visual acuity.

[a] Percentages of glaucomatous-appearing optic nerves are calculated from the subset of eyes (see row above) for which disk photographs were available within 24 months of the corresponding visual field.

[b] As described in the text, patients with AT1 (no focal defect) were considered glaucoma suspects in this analysis due to the absence of associated VF loss.